48th AIAA Aerospace Sciences Meeting Including the New Horizons Forum and Aerospace Exposition
4 - 7 January 2010, Orlando, Florida

AIAA 2010-1047

Simulation of Hypersonic Shock Wave/Boundary Layer Interaction Using High Order WENO Scheme

Yiqing Shen* Gecheng Zha† Manuel A. Huerta‡
University of Miami
Coral Gables, Florida 33124
E-mail: yqshen@miami.edu, gzha@miami.edu

Abstract

This paper investigates the accuracy and robustness of high order WENO schemes for predicting hypersonic shock wave/boundary layer interaction. The implicit time marching method with unfactored Gauss-Seidel line relaxation is used with a 5th order WENO finite difference scheme for inviscid fluxes. The viscous terms are discretized using a 4th order conservative central differencing. Numerical results agree well with the experiment of a hollow/flare geometry at Mach number of 12.49 and Reynolds number of $1.09 \times 10^5/ft$.

1 Introduction

Hypersonic aerothermodynamics is one of the most challenging issues of hypersonic propulsion system. The difficulties in simulating realistic high enthalpy hypersonic flows in wind tunnels testing have increased the demand to develop high fidelity computational fluid dynamics(CFD) methods for hypersonic flow applications. However, accurate prediction of shock wave/boundary layer interaction is very challenging, in particular, for heat transfer. Continuous efforts are needed to improve the hypersonic flow prediction accuracy.

For the numerical simulation of complicated hypersonic flowfields, it is required that the numerical schemes have the ability of shock capturing and fine-scale feature resolution. Due to the capability of capturing shock waves and the uniformly high order accuracy in the smooth regions, the WENO (weighted essentially non-oscillatory) schemes are a desirable option for hypersonic flows with shock waves.

The WENO scheme concept was first proposed by Liu et al[1] and then improved by Jiang and Shu[2]. Henrick et al[3] pointed out that the original smoothness indicators of Jiang and Shu fail to improving the accuracy order of WENO scheme at a critical point, where the first derivatives is zero. A mapping function is proposed by Henrick et al[3] to obtain the optimal order near critical points. Borges et al[4] devised a new set of WENO weights that satisfies the necessary and sufficient conditions for fifth-order convergence proposed by Henrick et al[3] and enhances the accuracy at critical points. Wang and Chen [5] proposed optimized WENO schemes for linear waves with discontinuity. Shen and Zha[6] found that most of all the WENO schemes do not obtain the optimal accuracy near discontinuities. They introduced fourth-order fluxes to overcome this drawback. For transonic flows, Shen et al [7] suggested to use an optimized ε in the smoothness estimators to achieve optimal weight in smooth regions in order to minimize dissipation. A class of higher than 5th order weighted essentially non-oscillatory schemes are designed by Balsara and

* Research Scientist, Dept. of Mechanical and Aerospace Engineering, AIAA Member
† Associate Professor, Dept. of Mechanical and Aerospace Engineering, AIAA Senior Member
‡ Professor, Dept. of Physics

Shu in [8]. Martin et al[9] proposed a symmetric WENO method by means of a new candidate stencil, the new schemes are $2r$th-order accurate and symmetric, and less dissipative than Jiang and Shu's scheme.

In 2001, there was a blind comparison between computational simulations and experimental data for hypersonic double-cone and hollow cylinder-flare flows[10, 11, 12, 13, 14, 15, 16, 17]. After that, there was a further comparison and analysis to explain the difference between the simulations and experiments[18, 19, 20, 21, 22]. In those simulations using Navier-Stokes equations, the TVD schemes are mainly used. TVD schemes will degrade the accuracy order at extrema in smooth region. WENO schemes have been applied to direct numerical simulation (DNS) and large eddy simulation (LES) of supersonic flows[9, 23, 24, 25]. But there are few research to investigate the accuracy and robustness of WENO schemes for predicting hypersonic flows.

The purpose of this paper is to investigate the accuracy and robustness of high order WENO schemes for predicting hypersonic flows. The implicit time marching method with unfactored Gauss-Seidel line relaxation is used with the high order WENO finite difference schemes for inviscid fluxes[7] to simulate the hypersonic flows. The viscous terms are discretized using a 4th order conservative central differencin[26]. The low Reynolds number hypersonic experiments conducted by Holden et al[21] are calculated in this paper. Since the flows are in laminar region, only the laminar Navier-Stokes equations are solved. The Numerical results agree well with the experiment.

2 Numerical Algorithm

2.1 Governing Equations

The normalized Navier-Stokes equations governing compressible viscous flows can be written in the Cartesian coordinate as:

$$\frac{\partial U}{\partial t}+\frac{\partial E}{\partial x}+\frac{\partial F}{\partial y}+\frac{\partial G}{\partial z}=\frac{1}{Re}\left(\frac{\partial R}{\partial x}+\frac{\partial S}{\partial y}+\frac{\partial T}{\partial z}\right) \tag{1}$$

where

$$U=\begin{bmatrix}\rho\\ \rho u\\ \rho v\\ \rho w\\ \rho e\end{bmatrix},\ E=\begin{bmatrix}\rho u\\ \rho u^2+p\\ \rho uv\\ \rho uw\\ (\rho e+p)u\end{bmatrix},\ F=\begin{bmatrix}\rho v\\ \rho uv\\ \rho v^2+p\\ \rho vw\\ (\rho e+p)v\end{bmatrix},\ G=\begin{bmatrix}\rho w\\ \rho uw\\ \rho vw\\ \rho w^2+p\\ (\rho e+p)w\end{bmatrix},$$

$$R=\begin{bmatrix}0\\ \tau_{xx}\\ \tau_{xy}\\ \tau_{xz}\\ u_k\tau_{xk}-q_x\end{bmatrix},\ S=\begin{bmatrix}0\\ \tau_{xy}\\ \tau_{yy}\\ \tau_{yz}\\ u_k\tau_{yk}-q_y\end{bmatrix},\ T=\begin{bmatrix}0\\ \tau_{xz}\\ \tau_{yz}\\ \tau_{zz}\\ u_k\tau_{zk}-q_z\end{bmatrix},$$

The repeated index k stands for the Einstein summation over x, y and z. The stress τ and heat flux q are,

$$\tau_{ik}=\mu\left[(\frac{\partial u_i}{\partial x_k}+\frac{\partial u_k}{\partial x_i})-\frac{2}{3}\delta_{ik}\frac{\partial u_j}{\partial x_j}\right]$$

$$q_j=\frac{-\mu}{(\gamma-1)M_\infty^2 Pr}\frac{\partial T}{\partial x_j}$$

The equation of state is

$$\rho e = \frac{p}{\gamma - 1} + \frac{1}{2}\rho(u^2 + v^2 + w^2)$$

In the above equations, ρ is density, u, v, and w are the Cartesian velocity components in x, y and z directions, p is static pressure, and e is total energy per unit mass, μ is molecular viscosity, J is the transformation Jacobian, γ, Re, M_∞, Pr *and* Pr_t are the ratio of specific heat, Reynolds number, freestream Mach number, Prandtl number and turbulent Prandtl number, respectively.

In the generalized computational coordinates, Eq.(1) can be written as:

$$\frac{\partial U'}{\partial t} + \frac{\partial E'}{\partial \xi} + \frac{\partial F'}{\partial \eta} + \frac{\partial G'}{\partial \zeta} = \frac{1}{Re}\left(\frac{\partial R'}{\partial \xi} + \frac{\partial S'}{\partial \eta} + \frac{\partial T'}{\partial \zeta}\right) \tag{2}$$

where,

$$U' = \frac{1}{J}U,$$

$$E' = \frac{1}{J}(\xi_t U + \xi_x E + \xi_y F + \xi_z G),$$

$$F' = \frac{1}{J}(\eta_t U + \eta_x E + \eta_y F + \eta_z G),$$

$$G' = \frac{1}{J}(\zeta_t U + \zeta_x E + \zeta_y F + \zeta_z G),$$

$$R' = \frac{1}{J}(\xi_x R + \xi_y S + \xi_z T),$$

$$S' = \frac{1}{J}(\eta_x R + \eta_y S + \eta_z T),$$

$$T' = \frac{1}{J}(\zeta_x R + \zeta_y S + \zeta_z T).$$

For simplicity, the prime $'$ in Eq.(2) will be omitted in the rest of this paper.

Eq.(2) is discretized in an implicit form as

$$\begin{gathered}\frac{1}{J\Delta t}\Delta U^{n+1} + (E^{n+1}_{i+\frac{1}{2}} - E^{n+1}_{i-\frac{1}{2}}) + (F^{n+1}_{j+\frac{1}{2}} - F^{n+1}_{j-\frac{1}{2}}) + (G^{n+1}_{k+\frac{1}{2}} - G^{n+1}_{k-\frac{1}{2}}) = \\ \frac{1}{Re}[(\tilde{R}^{n+1}_{i+\frac{1}{2}} - \tilde{R}^{n+1}_{i-\frac{1}{2}}) + (\tilde{S}^{n+1}_{j+\frac{1}{2}} - \tilde{S}^{n+1}_{j-\frac{1}{2}}) + (\tilde{T}^{n+1}_{k+\frac{1}{2}} - \tilde{T}^{n+1}_{k-\frac{1}{2}})]\end{gathered} \tag{3}$$

where, the inviscid numerical fluxes $E^{n+1}_{i+\frac{1}{2}}$, $F^{n+1}_{j+\frac{1}{2}}$ and $G^{n+1}_{k+\frac{1}{2}}$ are evaluated by the WENO scheme with a Riemann solver as described in Section 2.2-2.3, and the viscous numerical fluxes $\tilde{R}^{n+1}_{i+\frac{1}{2}}$, $\tilde{S}^{n+1}_{j+\frac{1}{2}}$ and $\tilde{T}^{n+1}_{k+\frac{1}{2}}$ are evaluated by a 4th order fully conservative central differencing described in Section 2.4.

2.2 Flux Difference Splitting

The Roe's flux difference scheme [27] is used as the Riemann solver with the WENO scheme in this paper. For the rest of the paper, we will take the flux in ξ direction as the example to explain the numerical methodology. Other directions can be obtained following the symmetric rule.

For the Roe scheme,

$$E_{i+\frac{1}{2}} = \frac{1}{2}[E(U^L) + E(U^R) - \tilde{A}(U^R - U^L)]_{i+\frac{1}{2}} \tag{4}$$

The high order accuracy of $E_{i+1/2}$ is obtained by achieving the high order accuracy of the left and right conservative variables U^L and U^R using the WENO scheme described below. This procedure is similar to the MUSCL scheme suggested by van Leer[28] and is adopted in both [7] and this paper.

2.3 The WENO Scheme[2]

The WENO scheme is used to evaluate the conservative variables U^L and U^R. The WENO scheme for a variable u^L can be written as:

$$u^L_{i+1/2} = \sum_{k=0}^{r} \omega_k q_k \tag{5}$$

where $\omega_k (k = 0, \cdots, r)$ are the weights, and the $q_k (k = 0, \cdots, r)$ are the rth order accuracy reconstruction of the variables in three different stencils.

$$\omega_k = \frac{\alpha_k}{\alpha_0 + \cdots + \alpha_{r-1}}, \tag{6}$$

where

$$\alpha_k = \frac{C_k}{(\varepsilon + IS_k)^p}, \quad k = 0, 1, 2 \tag{7}$$

where C_k are the optimal weights with the following values.

The smoothness indicators IS_k suggested by Jiang and Shu[2] are given by

$$IS_k = \sum_{l=1}^{r-1} \Delta x^{2l-1} \int_{x_{i-\frac{1}{2}}}^{x_{i+\frac{1}{2}}} (\frac{d^l}{dx^l} \hat{q}_k(x))^2 dx \tag{8}$$

The ε in Eq.(7) is introduced to avoid the denominator becoming zero. Jiang and Shu's numerical tests indicate that the results are not sensitive to the choice of ε as long as it is in the range of 10^{-5} to 10^{-7}. In their paper[2], ε is taken as 10^{-6}. In [7], Shen et al suggested to use an optimized ε value of $10^{-}2$ in the smoothness estimators to achieve optimal weight in smooth regions in order to minimize dissipation and improve convergence.

The u^R is constructed symmetrically as u^L about $i + 1/2$.

For the third-order($r = 2$) WENO scheme, there are

$$q_0 = -\frac{1}{2}u_{i-1} + \frac{3}{2}u_i, \quad q_1 = \frac{1}{2}u_i + \frac{1}{2}u_{i+1}$$

and

$$C_0 = 1/3, \quad C_1 = 2/3$$
$$IS_0 = (u_i - u_{i-1})^2, \quad IS_1 = (u_{i+1} - u_i)^2 \tag{9}$$

For the fifth-order($r = 3$) WENO scheme, there are

$$q_0 = \frac{1}{3}u_{i-2} - \frac{7}{6}u_{i-1} + \frac{11}{6}u_i$$

$$q_1 = -\frac{1}{6}u_{i-1} + \frac{5}{6}u_i + \frac{1}{3}u_{i+1}$$

$$q_2 = \frac{1}{3}u_i + \frac{5}{6}u_{i+1} - \frac{1}{6}u_{i+2}$$

and

$$C_0 = 0.1, \quad C_1 = 0.6, \quad C_2 = 0.3$$

and IS_k are

$$\begin{array}{l} IS_0 = \frac{13}{12}(u_{i-2} - 2u_{i-1} + u_i)^2 + \frac{1}{4}(u_{i-2} - 4u_{i-1} + 3u_i)^2 \\ IS_1 = \frac{13}{12}(u_{i-1} - 2u_i + u_{i+1})^2 + \frac{1}{4}(u_{i-1} - u_{i+1})^2 \\ IS_2 = \frac{13}{12}(u_i - 2u_{i+1} + u_{i+2})^2 + \frac{1}{4}(3u_i - 4u_{i+1} + u_{i+2})^2 \end{array} \tag{10}$$

2.4 The 4th-Order Schemes for Viscous Terms[26]

A set of fully conservative 4th-order accurate finite central differencing schemes using the same stencil width of the WENO scheme for the viscous terms is used in this paper. The scheme for the viscous derivative term $\frac{\partial R}{\partial \xi}$ in Navier-Stokes equations Eq.(2) can be written as the following,

$$\frac{\partial R}{\partial \xi}|_i = \frac{\tilde{R}_{i+1/2} - \tilde{R}_{i-1/2}}{\Delta \xi} \tag{11}$$

To obtain 4th order accuracy, $\tilde{R}$ needs to be reconstructed as

$$\tilde{R}_{i-1/2} = \sum_{I=i-3/2}^{i+1/2} \alpha_I R_I \tag{12}$$

where

$$\begin{array}{rl} \alpha_{i-3/2} = -\frac{1}{24},\ \alpha_{i-1/2} = \frac{26}{24},\ \alpha_{i+3/2} = -\frac{1}{24} & \\ R_{i-1/2} = [(\xi_x \tau_{xx}) + (\eta_y \tau_{xy}) + (\zeta_z \tau_{xz})]_{i-1/2} & \\ (\tau_{xx}) = & \mu\{\frac{4}{3}\left[(\xi_x \frac{\partial u}{\partial \xi}) + (\eta_x \frac{\partial u}{\partial \eta}) + (\zeta_x \frac{\partial u}{\partial \zeta})\right] \\ & -\frac{2}{3}[(\xi_y \frac{\partial v}{\partial \xi}) + (\eta_y \frac{\partial v}{\partial \eta}) + (\zeta_y \frac{\partial v}{\partial \zeta}) \\ & (\xi_z \frac{\partial w}{\partial \xi}) + (\eta_z \frac{\partial w}{\partial \eta}) + (\zeta_z \frac{\partial w}{\partial \zeta})]\} \end{array} \tag{13}$$

If R_I in Eq.(12) can be approximated with the accuracy order not lower than 4th order, the Taylor expansion analysis of (11) and (12) will give the following relation[26],

$$\frac{1}{\Delta \xi}(\tilde{R}_{i+1/2} - \tilde{R}_{i-1/2}) = R^{'}(\xi_i) + O(\Delta \xi^4) \tag{14}$$

i.e. the 4th order accuracy is achieved.

In order to achieve the highest order accuracy of R_I with $I = i-3/2, i-1/2, i+1/2$, the approximation of each component in Eq. (12) using all the involved points of the WENO stencil is given below:

$$\mu_I = \sum_{l=m}^{n} C_l^I \mu_{i+l}, \tag{15}$$

$$\frac{\partial u}{\partial \xi}|_I = \frac{1}{\Delta \xi} \sum_{l=r}^{s} D_l^I u_{i+l}, \tag{16}$$

$$\frac{\partial u}{\partial \eta}|_I = \sum_{l=m}^{n} C_l^I \frac{\partial u}{\partial \eta}|_{i+l,j} \tag{17}$$

where

$$\frac{\partial u}{\partial \eta}|_{i,j} = \frac{1}{\Delta \eta} \sum_{l=p}^{q} C_l^c u_{i,j+l}, \tag{18}$$

By choosing different ranges for $(m,n),(r,s),(p,q)$ and different coefficients C_l^I, D_l^I, C_l^c, one can obtain different order accuracy approximation to the viscous terms. The principle of choosing $(m,n),(r,s),(p,q)$ is to ensure that the approximation of $\frac{\partial R}{\partial \xi}|_i$ in Eq.(11) is a central differencing. For example, in this paper, $(m,n)=(-2,1),(r,s)=(-3,2), and\ (p,q)=(-2,2)$ are used, and they give[26],

$$\mu_I = \sum_{l=m}^{n} C_l^I \mu_{i+l} + O(\Delta\xi^4), \tag{19}$$

$$\frac{\partial u}{\partial \xi}|_I = \frac{1}{\Delta\xi}\sum_{l=r}^{s} D_l^I u_{i+l} + O(\Delta\xi^5), \tag{20}$$

$$\frac{\partial u}{\partial \eta}|_I = \sum_{l=m}^{n} C_l^I \frac{\partial u}{\partial \eta}|_{i+l,j} + O(\Delta\xi^4, \Delta\eta^4), \tag{21}$$

where

$$\frac{\partial u}{\partial \eta}|_{i,j} = \frac{1}{\Delta\eta}\sum_{l=p}^{q} C_l^c u_{i,j+l} + O(\Delta\eta^4) \tag{22}$$

the coefficients C_l^I, D_l^I, C_l^c can be obtained by Taylor's series expansion and are given in Tables 1-3.

Table 1: The coefficients of C_l^I

I	C_{-2}^I	C_{-1}^I	C_0^I	C_1^I
$i-3/2$	5/16	15/16	-5/16	1/16
$i-1/2$	-1/16	9/16	9/16	-1/16
$i+1/2$	1/16	-5/16	15/16	5/16

Table 2: The coefficients of D_l^I

I	D_{-3}^I	D_{-2}^I	D_{-1}^I	D_0^I	D_1^I	D_2^I
$i-3/2$	71/1920	-141/128	69/64	1/192	-3/128	3/640
$i-1/2$	-3/640	25/384	-75/64	75/64	-25/384	3/640
$i+1/2$	-3/640	3/128	-1/192	-69/64	141/128	-71/1920

Table 3: The coefficients of C_l^c

C_{-2}^c	C_{-1}^c	C_0^c	C_1^c	C_2^c
1/12	-8/12	0	8/12	-1/12

Shen et al [26] proved that the scheme of Eq. (11) is symmetric with respect to cell i and is of 4th-order accuracy. The symmetry of Eq. (11) satisfies the diffusion property of viscous fluxes.

2.5 Time Marching Method

The unfactored implicit Gauss-Seidel line relaxation method developed in[29, 30, 31, 32] by the authors' research group is adopted in this paper.

The implicit fluxes given in Eq. (3) are treated as the following: The inviscid fluxes defined by Eq. (4) are expanded in Taylor's series about interface $i+1/2$,

$$E^L_{i+1/2}|^{n+1} = E^L_{i+1/2}|^n + (\frac{\partial E}{\partial U}|^L_{i+1/2})|^n \Delta U^L_{i+1/2}|^{n+1}$$
$$= E^L_{i+1/2}|^n + A^L_{i+\frac{1}{2}}|^n \Delta U^L_{i+1/2}|^{n+1}$$
$$E^R_{i+1/2}|^{n+1} = E^R_{i+1/2}|^n + (\frac{\partial E}{\partial U}|^R_{i+1/2})|^n \Delta U^R_{i+1/2}|^{n+1}$$
$$= E^R_{i+1/2}|^n + A^R_{i+\frac{1}{2}}|^n \Delta U^R_{i+1/2}|^{n+1}$$

and,

$$\tilde{A}(U^R - U^L)|^{n+1}_{i+1/2} =$$
$$\tilde{A}(U^R - U^L)|^n_{i+1/2} + \tilde{A}_{i+1/2}|^n (\Delta U^R_{i+1/2}|^{n+1} - \Delta U^L_{i+1/2}|^{n+1})$$

The first-order approximation is used for the implicit convective terms to enhance diagonal dominance. That is:

$$\Delta U^L_{i+1/2}|^{n+1} = \Delta U^{n+1}_i, \quad \Delta U^R_{i+1/2}|^{n+1} = \Delta U^{n+1}_{i+1}$$

The fluxes F and G are treated in the same way. The implicit viscous fluxes R, S and T are discretized using 2nd order central differencing. Then the final implicit form is the following,

$$\bar{B}\Delta U^{n+1}_{i,j,k} + A^+\Delta U^{n+1}_{i+1,j,k} + A^-\Delta U^{n+1}_{i-1,j,k} + B^+\Delta U^{n+1}_{i,j+1,k} + B^-\Delta U^{n+1}_{i,j-1,k} +$$
$$C^+\Delta U^{n+1}_{i,j,k+1} + C^-\Delta U^{n+1}_{i,j,k-1} = RHS^n \tag{23}$$

The Gauss-Seidel line iteration in a certain sweep direction, for example, in ξ direction assuming the sweeping from small index value to large one, can be written as

$$B^-\Delta U^{n+1}_{i,j-1,k} + \bar{B}\Delta U^{n+1}_{i,j,k} + B^+\Delta U^{n+1}_{i,j+1,k} = RHS' \tag{24}$$

where,

$$RHS' = RHS^n - A^+\Delta U^n_{i+1,j,k} - A^-\Delta U^{n+1}_{i-1,j,k} - C^+\Delta U^n_{i,j,k+1} - C^-\Delta U^{n+1}_{i,j,k-1} \tag{25}$$

The accuracy of the converged solution is controlled by RHS of Eq. (23), which is calculated by the 5th order WENO scheme for inviscid fluxes described in section 2.2-2.4 and the conservative 4th order central differencing for viscous terms described in [7]. The overall accuracy of a converged solution is therefore 4th order.

3 Results and Discussion

In this paper, the case of Run9 of the hollow cylinder/flare[21] is calculated. The Mach number is 12.49, Reynolds number is $1.09 \times 10^5/ft$. One half of the flow field is calculated due to the symmetry of the flow field with the mesh of $518 \times 120 \times 40$. Both the 3rd order and 5th order WENO schemes are used to test their performance. The viscous terms are discretized using the same 4th order central differencing.

Fig. 1 is the pressure distribution on the wall for the cylinder/flare configuration. Fig. 2[21] is the experimental schlieren photo and density contour of Gnoffo. Fig. 3 is density contour obtained by WENO-5 scheme. They agree very well with the experiment. Fig. 3 shows that there are two discontinuities. One is parallel and very close to the wall, the other is the reflect shock wave. Fig. 4 is the density and pressure distribution at $x/L = 1.8$ across the flow field from the wall. Fig. 4 indicates that there is a large jump

for pressure and density when the flow is crossing the reflect shock. Across the 2nd discontinuity near the wall, the density has a large change, and the pressure jump is mild. This may indicate that the 2nd discontinuity is similar to a slip line or contact discontinuity.

Figs. 5 and 6 show the pressure coefficients and the Stanton number on the wall surface. It can be seen that the result of the WENO-5 agrees excellently with the experiment. The WENO-3 also obtains good results, but its separated region is smaller than that of the experiment and the WENO-5 scheme, and lowest pressure point is slightly ahead to the WENO-5 and experiment. It is worthy pointing out that the computed flow field behind $x/L = 1.7$ using the WENO-5 is unstable, the flow field is always oscillatory with small amplitude in the region near the exit of the cone. The experimental measurement also shows some oscillation. It is not clear if such instability is numerical or physical. More study is needed to investigate this phenomenon.

4 Conclusions

The 3rd order and 5th order WENO schemes for convective terms and 4th-order central differencing for viscous terms are employed to predict hypersonic shock wave/boundary layer interaction flow. The flow with high Mach numner of 12.49 over a hollow cylinder/flare configuration is simulated. Numerical results agree excellently with the experiment. The 5th-order WENO schemes is significantly more accurate than the 3rd-order WENO scheme, for prediction of the separate region, pressure coefficients and heat transfer coefficient on the wall. It is also found that the flow in the region behind the reflective shock wave and near the wall is unstable by using the 5th-order WENO scheme.

5 Acknowledgment

This research is funded by AFOSR grant FA9550-09-1-0105.

References

[1] X.D. Liu, S. Osher, and T. Chan, "Weighted essentially non-oscillatory schemes," *J.Comput.Phys.*, vol. 115, pp. 200–212, 1994.

[2] G.S. Jiang, and C.W. Shu, "Efficient implementation of weighted ENO schemes," *J.Comput.Phys.*, vol. 126, pp. 202–228, 1996.

[3] A.K. Henrick, T.D. Aslam, J.M. Powers, "Mapped weighted essentially non-oscillatory schemes:Achiving optimal order near critical points," *J.Comput.Phys.*, vol. 208, pp. 206–227, 2005.

[4] R. Borges, M. Carmona, B. Costa and W.S. Don, "An improved weighted essentially non-oscillatory scheme for hyperbolic conservation laws," *Journal of Computational Physics*, vol. 227, pp. 3191–3211, 2008.

[5] Z.J. Wang and R.F. Chen, "Optimized weighted essentially non-oscillatory schemes for linear waves with discontinuity," *J.Comput.Phys.*, vol. 174, pp. 381–404, 2001.

[6] Y. Q. Shen and G. C. Zha, "Improvement of weighted essentially non-oscillatory schemes near discontinuity." AIAA paper 2009-3655, 2009.

[7] Y.-Q. Shen, G.-C. Zha, and B.-Y. Wang, "Improvement of Stability and Accuracy of Implicit WENO Scheme," *AIAA Journal*, vol. 47, pp. 331–344, 2009.

[8] D.S. Balsara and C.-W. Shu, "Monotonicity Preserving weighted essentially non-oscillatory schemes with increasingly high order of accuracy," *J.Comput.Phys.*, vol. 160, pp. 405–452, 2000.

[9] M. P. Martin, E. M. Taylor, M. Wu, and V. G. Weirs, "A Bandwidth-Optimized WENO Scheme for the Direct Numerical Simulation of Compressible Turbulenc," *Journal of Computational Physics*, vol. 220, pp. 270–289, 2006.

[10] Candler, G. V., and Nompelis, I., and Druguet, M-C, "Navier-Stokes predictions of hypersonic double-cone and cylinder-flare flow fields." AIAA-2001-1024, Jan. 2001.

[11] Gnoffo, P. A., "CFD Validation Studies for Hypersonic Flow Prediction." AIAA-2001-1025, Jan. 2001.

[12] J. Moss, "DSMC Computations for Regions of Shock/Shock and Shock/Boundary Layer Interaction." AIAA-2001-1027, Jan. 2001.

[13] Kato, H., and Tannehill, J. C., "Computation of Hypersonic Laminar Separated Flows using an Iterated PNS Algorithm." AIAA-2001-1028, Jan. 2001.

[14] Boyd, I. D., and Wang, W-L, "Monte Carlo Computations of Hypersonic Interacting Flows." AIAA-2001-1029, Jan. 2001.

[15] Roy, C. J., and Bartel, T. J., and Gallis, M. A., and Payne, J. L., "DSMC and Navier-Stokes Predictions for Hypersonic Laminar Interacting Flows." AIAA-2001-1030, Jan. 2001.

[16] Holden, M. S., and Wadhams, T. P., "Code Validation Study of Laminar Shock/Boundary Layer and Shock/Shock Interactions in Hypersonic Flow, Part A: Experimental Measurements." AIAA-2001-1031, Jan. 2001.

[17] Harvey, J. K., and Holden, M. S., and Wadhams, T. P., "Code Validation Study of Laminar Shock/Boundary Layer and Shock/Shock Interactions in Hypersonic Flow, Part B: Comparison with Navier-Stokes and DSMC Solutions." AIAA-2001-1031, Jan. 2001.

[18] J. N. Moss, "Hypersonic flows about a 25^o sharp cone." NASA TM-2001-211253, Dec. 2001.

[19] Candler,G. V., and Nompelis, I., and Druguet, M-C, and Holden, M. S., and Wadhams, T. P., and Boyd, I. D., and Wang, W-L, "CFD Validation for Hypersonic Flight: Hypersonic Double-Cone Flow Simulations." AIAA-2002-0581, Jan. 2002.

[20] Roy, C. J., and Gallis, M. A., and Bartel, T. J., and Payne J. L., "Navier-Stokes and DSMC Simulations for Hypersonic Laminar Shock-Shock Interaction Flows." AIAA-2002-0737, Jan. 2002.

[21] Holden, M. S., and Wadhams, T. P., and Harvey, J. K., and Candler, G. V., "Comparisons Between DSMC and Navier-Stokes Solutions and Measurements in Regions of Laminar Shock Wave Boundary Layer Interaction in Hypersonic Flows." AIAA-2002-0435, Jan. 2002.

[22] Holden, M. S., and Wadhams, T. P., and Harvey, J. K., "Experimental Studies for NS & DSMC Code Validation for Laminar Hypervelocity Flows." AIAA-2003-3641, June 2003.

[23] D. J. Hill, D. I. Pullin, " Hybrid tuned center-difference-WENO method for large eddy simulations in the presence of strong shock," *Journal of Computational Physics*, vol. 194, pp. 435–450, 2004.

[24] Wu, M., and Martin, M.P., "Direct Numerical Simulation of Shockwave and Turbulent Boundary Layer Interaction over a Compression Ramp," *AIAA Journal*, vol. 45, pp. 879–889, 2007.

[25] Chi-Wang Shu, "High Order Weighted Essentially Nonoscillatory Schemes for Convection Dominated Problems," *SIAM Review*, vol. 51, pp. 82–126, 2009.

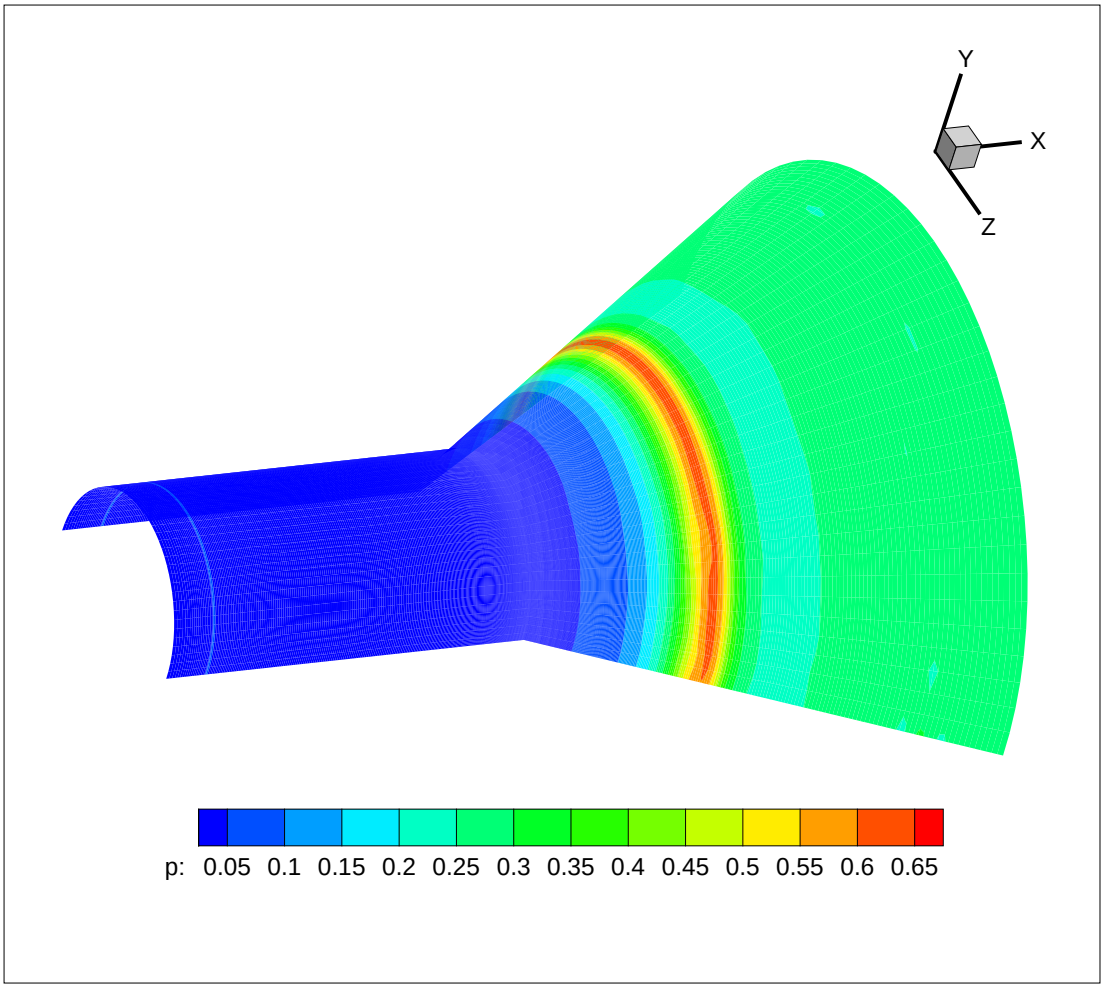

Figure 1: Pressure contours on wall, the WENO-5 scheme

[26] Y. Q. Shen, G. Z. Zha, X. Y. Chen , "High order conservative differencing for viscous terms and the application to vortex-induced vibration flows," *Journal of Computational Physics*, vol. 228, pp. 8283–8300, 2009.

[27] P. Roe, "Approximate Riemann Solvers, Parameter Vectors, and Difference Schemes," *Journal of Computational Physics*, vol. 43, pp. 357–372, 1981.

[28] B. Van Leer, "Towards the Ultimate Conservative Difference Scheme, III," *Journal of Computational Physics*, vol. 23, pp. 263–75, 1977.

[29] Z. Hu, G. -C Zha, "Calculations of 3D compressible using an efficient low diffusion upwind scheme," *International Journal for Numerical Methods in Fluids*, vol. 47, pp. 253–269, 2005.

[30] Z. J. Hu, " Parallel computation of fluid-structural interactions using high resolution upwind schemes." Ph.D. Thesis, Dept. of Mech. Aero. Eng., Univ. of Miami, May 2005.

[31] X. Chen, G. -C Zha, "Fully coupled fluid-structural interactions using an efficient high solution upwind scheme," *Journal of Fluid and Structure*, vol. 20, pp. 1105–1125, 2005.

[32] Y.Q. Shen, B.Y. Wang,and G.C. Zha, "Comparison Study of Implicit Gauss-Seidel Line Iteration Method for Transonic Flows." AIAA-2007-4332, June 2007.

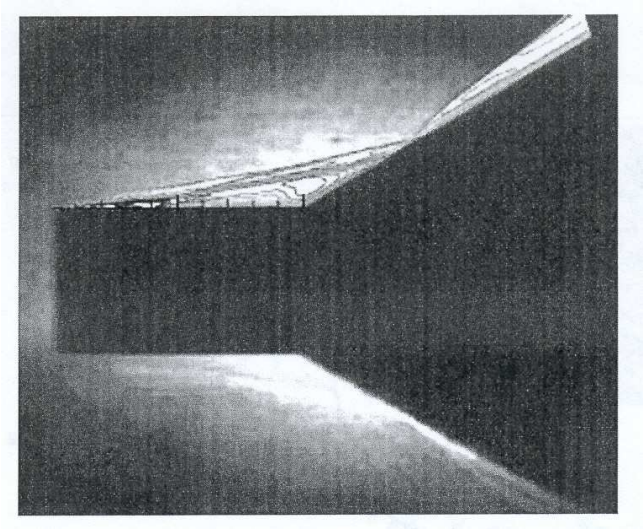

Figure 2: Schlieren photo with density contour of Gnoffo[21]

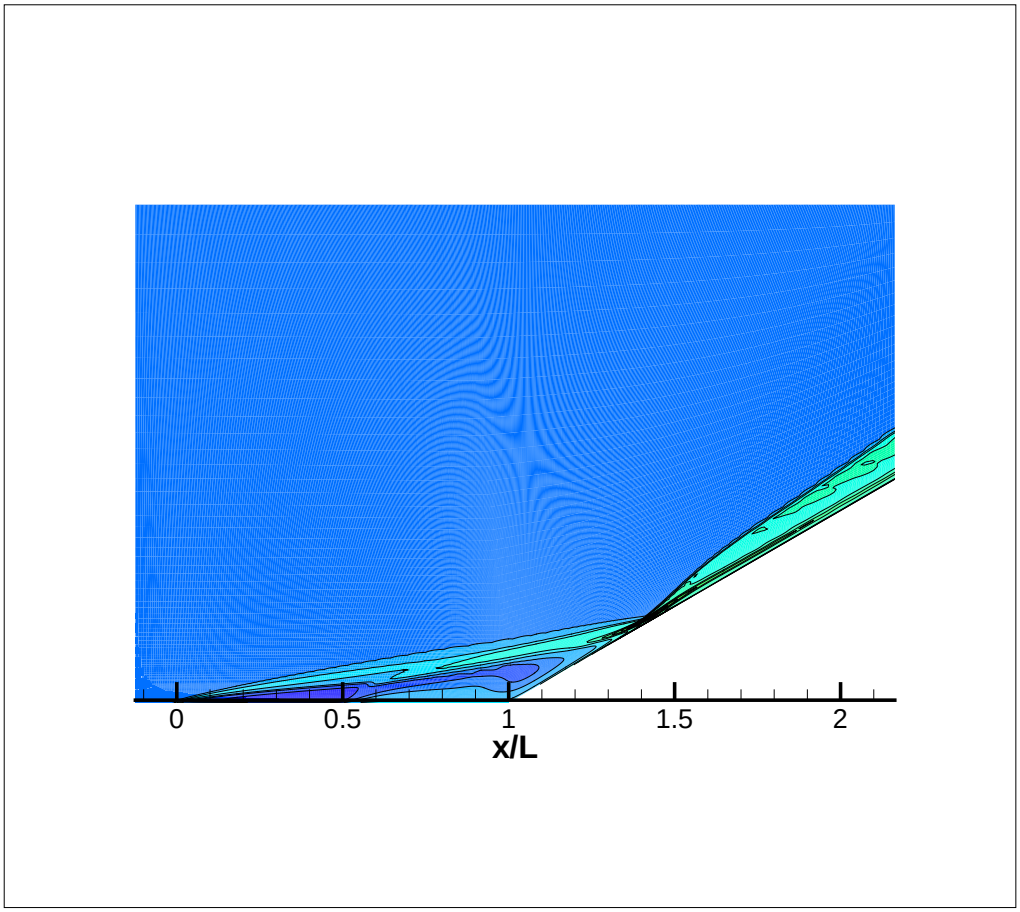

Figure 3: Density contours, the WENO-5 scheme

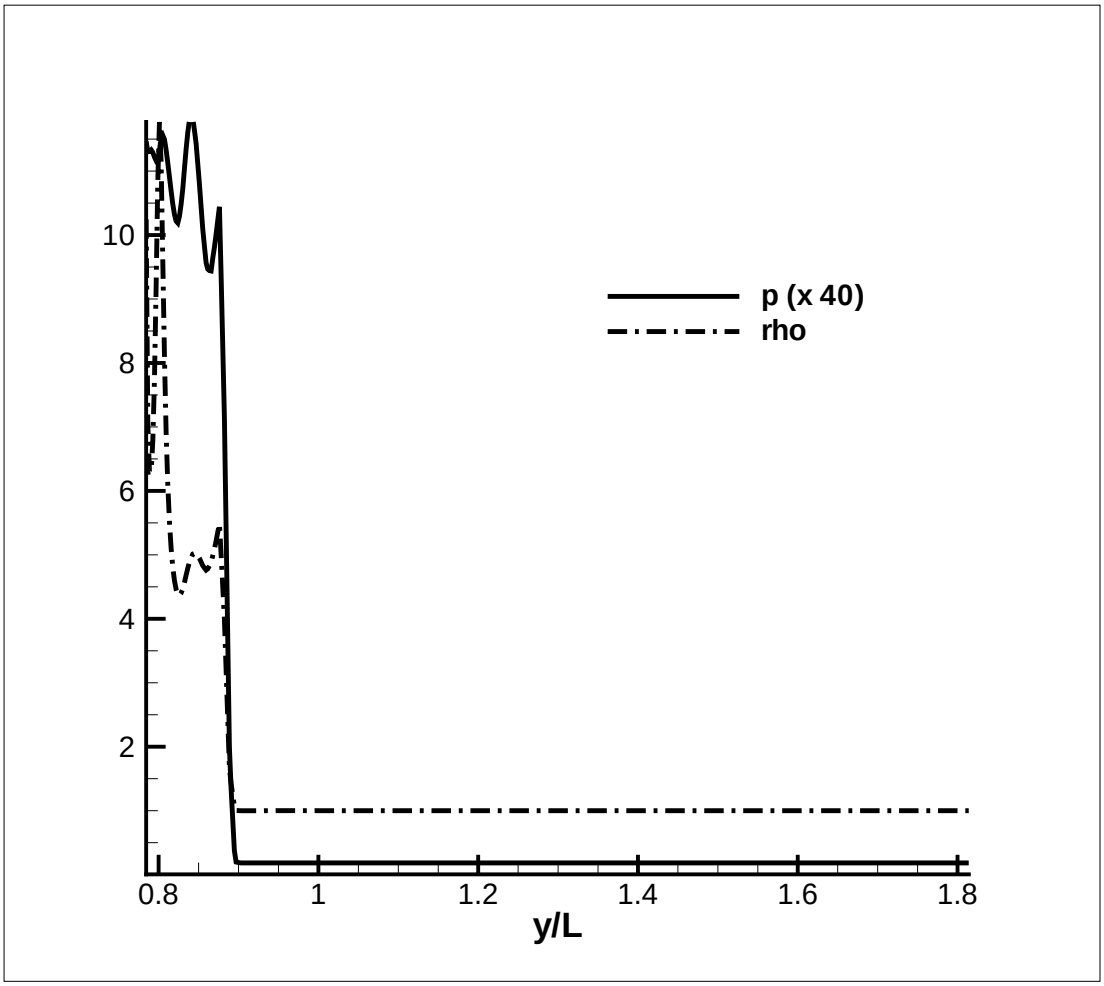

Figure 4: Density and pressure distribution at $x/L = 1.8$, the WENO-5 scheme

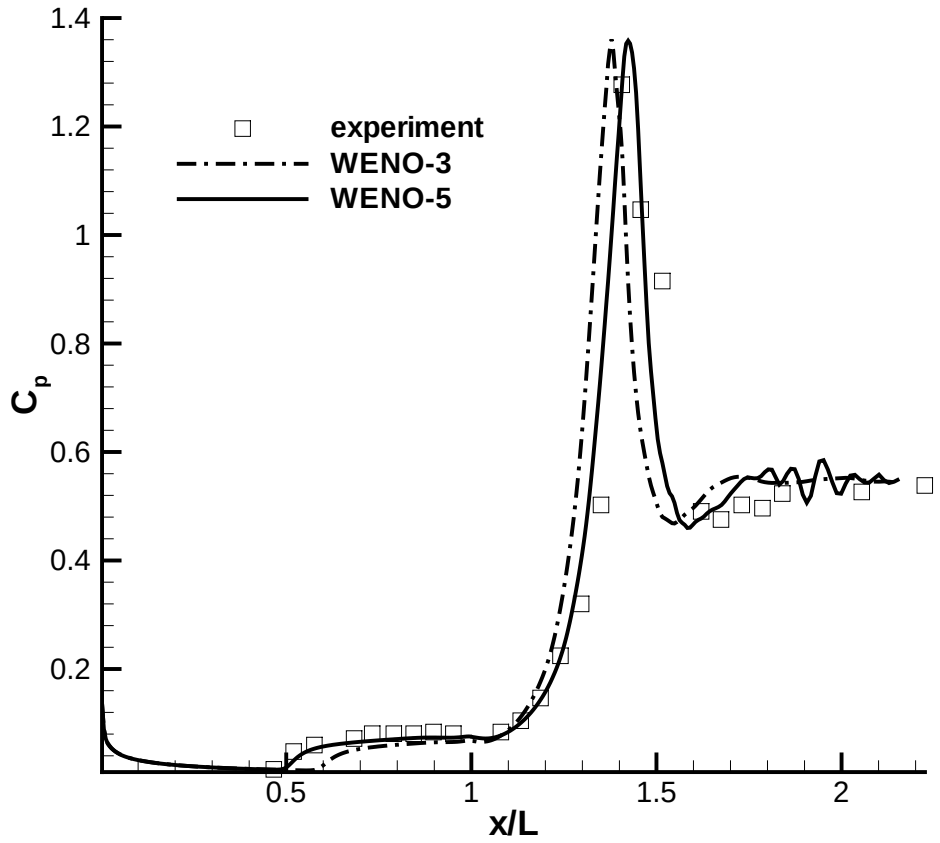

Figure 5: Pressure coefficient distribution on wall

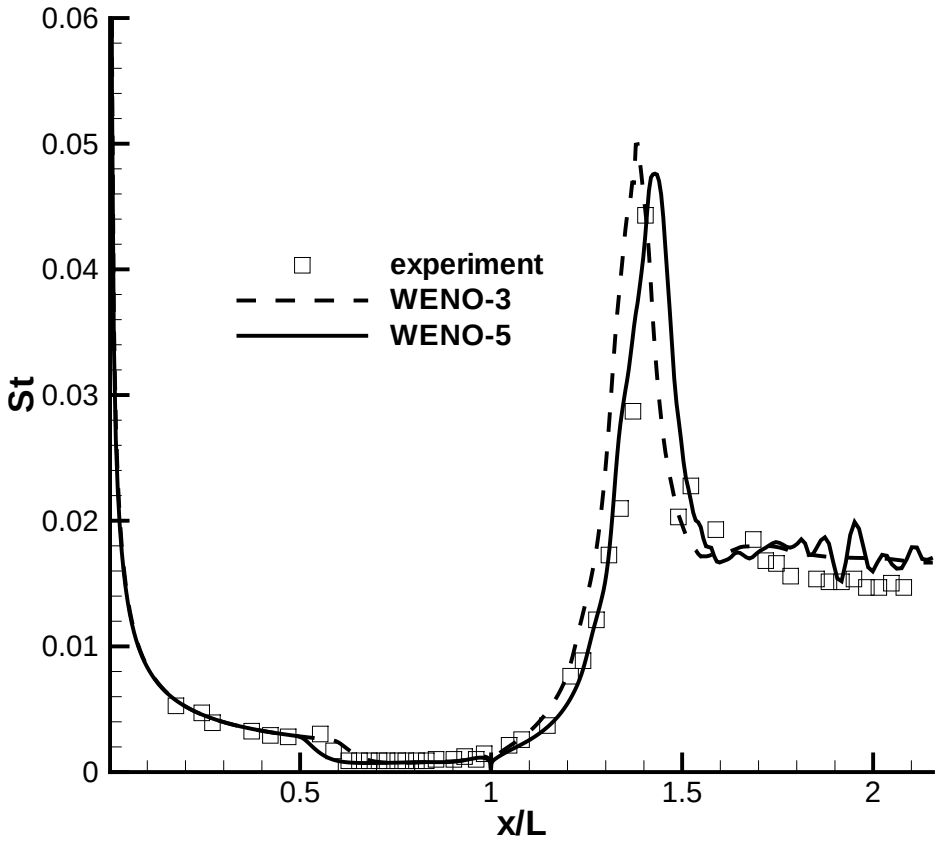

Figure 6: Stanton number distribution on wall